Journal of Statistical Physics, Vol. 114, Nos. 5/6, March 2004 (© 2004)

Invasion and Extinction in the Mean Field Approximation for a Spatial Host-Pathogen Model

M. A. M. de Aguiar,[1,2] E. M. Rauch,[1,3] and Y. Bar-Yam[1,4]

Received February 4, 2003; October 2, 2003

We derive the mean field equations of a simple spatial host-pathogen, or predator-prey, model that has been shown to display interesting evolutionary properties. We compare these equations, and the equations including pair-correlations, with the low-density approximations derived by other authors. We study the process of invasion by a mutant pathogen, both in the mean field and in the pair approximation, and discuss our results with respect to the spatial model. Both the mean field and pair correlation approximations do not capture the key spatial behaviors—the moderation of exploitation due to local extinctions, preventing the pathogen from causing its own extinction. However, the results provide important hints about the mechanism by which the local extinctions occur.

KEY WORDS: Evolution; predator-prey; host-pathogen; mean-field; spatial.

1. INTRODUCTION

The importance of space in ecology, evolution and epidemiology has become increasingly recognized in recent research. It has become apparent that inhomogeneities in spatially distributed populations can fundamentally change the dynamics of these systems.[1–5] In particular, spatial symmetry breaking and the resulting patterns of inhomogeneity lead to dynamic

[1] New England Complex Systems Institute, Cambridge, Massachusetts 02138.
[2] Instituto de Física Gleb Wataghin, Universidade Estadual de Campinas, 13083-970 Campinas, São Paulo, Brazil; e-mail: aguiar@ifi.unicamp.br
[3] MIT Artificial Intelligence Laboratory, 200 Technology Square, Cambridge, Massachusetts 02139.
[4] Department of Molecular and Cellular Biology, Harvard University, Cambridge, Massachusetts 02138.

0022-4715/04/0300-1417/0 © 2004 Plenum Publishing Corporation

behaviors that are qualitatively different from aggregate (homogeneous) models. These changes affect not only our models of the rate of change of system variables, but also our basic understanding of what is and is not important in describing these systems.

Space can be taken into account in essentially three different ways: continuous partial differential equations, patch models and lattice models. The first class includes reaction-diffusion equations, used to model pigment patterns in animal skins[6] and ecological processes.[7] Patch models, or structured population models, assume an a priori spatial distribution of the population into clusters, or demes, that *weakly* interact via migration or other types of contact. Each cluster is assumed to be uniform. The vast literature on this subject can be traced from ref. 8. Due to the assumption of weak interactions, many of the more interesting dynamic spatial effects were not studied in this context. Finally, lattice models treat space as a discrete set of sites, or regions, whose states are determined by local interaction with nearby points. These interactions are generally not limited to weak interactions, and the class of behaviors that can be studied are similar to those of partial differential equations. Spatial patterns of inhomogeneity may form spontaneously in lattice models, depending on the specifics of the model and parameters.

A simple lattice host-pathogen or predator-prey model has become a paradigm for the study of spatially extended dynamics. This model was first introduced by Tainaka.[9] In epidemiology, the model was introduced by Comins *et al.*[10] and further studied in refs. 11–14. In this model, it is possible for predators or pathogens to overexploit their prey or hosts, thereby eventually causing their own extinction. However, when predators or pathogens can mutate, they evolve to moderate values of exploitation of the prey or hosts. Recent studies have revealed that this occurs because of the local extinction of overexploitative strains many generations after they first arise.[4, 5] The salient features of the model are local reproduction of both host and pathogen, and the killing off of infected hosts by pathogens. The model is a probabilistic cellular automaton, in which the state of each site is updated probabilistically according to the state of nearby sites. The system is known to exhibit a very rich and complex dynamical behavior. Some insight in the role of the parameters and global behavior of the system can be obtained from the mean field approximation. The mean field equations correspond to the homogeneous version of the model, that is, when all hosts and pathogens experience the same local environment. This is generally a very crude approximation, and at least pair correlations must be taken into account in order to obtain more features of the spatial model. Still, the mean field provides an important starting point for conceptual as well as better analytic discussions of spatial effects.

The mean field equations for the host-pathogen model were first presented by Rand *et al.*[13] (see also refs. 15–17). Corrections due to pair correlations were considered in ref. 16. Satulovsky and Tomé[18] have also derived the mean field and pair correlation equations for a similar model. In this paper we argue that the mean field equations and the pair approximation in refs. 13 and 15–17 are actually only approximations to the correct equations. In the derivation of these equations it is assumed that the time interval between updates is very small, so that the discrete time updates of the cellular automaton can be replaced by continuous time differential equations. As we shall discuss in Section 3, without considering the way discrete transitions are aggregated, there is no unique way of making this transition. The continuous time limit adopted in this paper takes into account that the action of one agent, like a susceptible host replicating into a neighboring site, does interfere with the actions of the other neighboring agents. As an example, if an agent replicates into a site, no other neighboring agent can replicate there. When all replications are counted to determine the rate of population change by replication onto empty sites from multiple adjacent sites, the interference is significant, and therefore it is relevant in the continuous time differential equations. In the derivations of the mean field equations in previous works, refs. 13 and 15–17, these interferences were neglected. As a result, the probability of infection of a susceptible host by an infected individual is overcounted, as is the probability of a susceptible host being born on a empty site. Their equations are strictly valid only in the low density limit and possibly for small rates of transmissibility of the pathogen and for small birth rates of susceptible hosts, when these overcountings are not important. We note that the model in ref. 18 assumes the type of overcounting discussed above even in the lattice (simulation) version. The mean field and pair approximation equations derived there are, therefore, consistent and correct, although the model itself is not very realistic.

A demonstration of the correctness of our equations can be performed by considering a simple cellular automaton where the lattice sites can be only either empty or occupied by a host. This is a useful test, because, unlike for the full host-pathogen model, the mean field is a good approximation over a wide range of parameters. The results, plotted in Fig. 1, show that the accuracy of our mean field equation of the average number of hosts is much superior to that of the approximate equations previously obtained by others.

In order to further clarify this point we first consider a discrete version of the mean field limit, without taking the limit of small time interval between updates. This provides a well defined mean field approximation and can be compared both to the original cellular automaton and to the

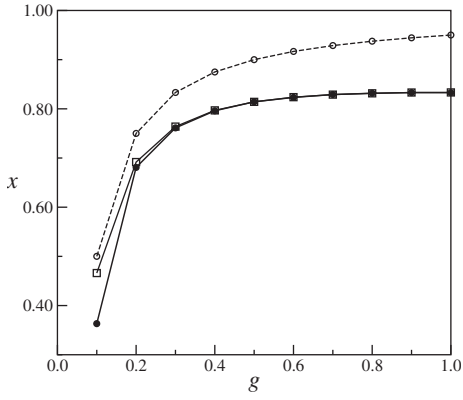

Fig. 1. Comparison between the average population of hosts (x) for a model of host reproduction and death. Reproduction occurs at a rate g and death occurs at the rate $\mu = 0.2$. Filled circles show the lattice simulations (thick solid line), squares show the exact mean field calculations we derive in this paper given by Eq. 30 (solid thin line), and empty circles show the approximate mean field calculations as reported previously by others and given by Eq. (31) (dashed line).

continuous time differential equations. We find that the discrete mean field agrees very well our continuous time mean field equations and not well with previously derived continuous time ones. In particular, the discrete and continuum equations give identical results at equilibrium.

The correct continuous time mean field equations for the full host-pathogen model were recently presented in ref. 19. In this paper we present a detailed derivation of these equations and compare them with the approximate ones. Using the new results we consider implications for our understanding of evolutionary processes in this model. In particular, we discuss the question of invasion of a population by mutant pathogens. When mutant types with different transmissibilities can arise in the lattice model, there is an evolutionarily stable type which cannot be invaded by types with lower and (sometimes) higher transmissibilities. This problem was studied in refs. 4, 5, 14, and 20–22 in the context of lattice models and in refs. 13, 15, and 17 in the mean field limit using their approximate equations. Here we derive the full mean field and pair approximation limit for the case of two types of pathogen. We show, as had been already shown with the approximate equations, that the mean field limit cannot account for the invasion features observed in the spatial model. Even including pair correlations, the equations fail to describe the emergence of an evolutionarily stable pathogen type. However, we show that the dynamics

in the pair approximation does give us hints about how intermediate-transmissibility types are resistant to invasion by higher-transmissibility ones.

The paper is organized as follows: in Section 2 we describe the lattice model and in Section 3 we derive its master equation. In Section 4 we obtain the mean field equations for one and two types of pathogen. Section 5 is devoted to the pair approximation for the case of a single type of pathogen and Section 6 considers the pair approximation for two pathogens and the process of invasion. A discussion on the dynamics of invasion in the pair approximation versus the corresponding behavior in the lattice model is presented in Section 7, where we also summarize our conclusions.

2. THE MODEL

We consider a two-dimensional spatial lattice with $N = \tilde{N} \times \tilde{N}$ sites. The state of each site can be either empty (0), occupied by a susceptible (S), or occupied by an infected individual (I_τ). Alternately, each cell can be considered to represent local populations, either absent or at carrying capacity. At each time step, the susceptible hosts reproduce into each nearby cell with probability g if that cell is not yet occupied. The probability of reproduction is independent for each neighbor. An infected host dies with probability v, the virulence. Finally an infected host I_τ causes a neighboring uninfected host to become infected with probability τ, the transmissibility. The subscript τ allows more than one type to be present on the lattice. For the sake of simplicity we shall re-label the state (S) as (1) and (I_τ) as (τ).

The state of the system is denoted by $\sigma = (\sigma_1, \sigma_2, ..., \sigma_N)$, where σ_i is the state at the ith site. We call $\omega_i(\sigma)$ the transition probability per unit time of the state at the site i. The transition probabilities are:

$$\omega_i(\sigma) = \begin{cases} 1-(1-g)^{n_i} & \text{if} \quad \sigma_i = 0 \\ 1-(1-\tau)^{m_i} & \text{if} \quad \sigma_i = 1 \\ v & \text{if} \quad \sigma_i = \tau \end{cases} \tag{1}$$

where $n_i = \sum_j \delta(\sigma_{i+j}, 1)$ is the number of susceptible neighbors to i, and $m_i = \sum_j \delta(\sigma_{i+j}, \tau)$ is the number of infected neighbors to i. The sum over j runs through all the nearest neighbors. We call ζ the total number of nearest neighbors, which is usually taken to be 2 for one-dimensional lattices and 4 for two-dimensional lattices. Note that, since a susceptible cannot be infected twice, the probability of becoming infected has to be calculated as "one minus the probability of not becoming infected." This gives rise to the term $1-(1-\tau)^{m_i}$. Similarly, an empty site can become occupied only by

offspring of a single susceptible neighbor host, thus the term $1-(1-g)^{n_i}$. Note also that the transitions between states are being defined as cyclic: $0 \to 1 \to \tau \to 0$.

Allowing for the simultaneous existence of different types of pathogens, and mutation between the types, enables the study of evolutionary dynamics, where different types compete for the same susceptibles. The transmissibility becomes a quantitative trait of an individual pathogen. When a pathogen of transmissibility τ reproduces, its offspring has probability μ of having transmissibility $\tau \pm \epsilon$. For simplicity we assume that τ may take only discrete values $\tau_k = k\epsilon$, $k = 1, 2, ..., M$ where $M = 1/\epsilon$. The state occupied by a host infected with pathogen τ_k will be labeled (τ_k).

When more than one type of pathogen is present, the transition probability per unit time of the state at the site i is written as $\omega_{ik}(\sigma)$. The possible (cyclic) transitions are: from (0) to (1), from (1) to (τ_k) and from (τ_k) to (0). The transition probabilities are given by

$$\omega_{ik}(\sigma) = \begin{cases} 1-(1-g)^{n_i} & \text{if} \quad \sigma_i = 0 \\ \Omega_k & \text{if} \quad \sigma_i = 1 \\ v & \text{if} \quad \sigma_i = \tau_{k'} \qquad \text{for all } k' \end{cases} \tag{2}$$

where Ω_k is the probability that susceptible hosts become infected by the pathogen with transmissibility τ_k:

$$\Omega_k = \chi \left[\frac{\mu}{2} p_{k-1} + \frac{\mu}{2} p_{k+1} + (1-\mu)\, p_k \right] \tag{3}$$

with

$$\chi = \frac{1-\prod_j (1-\tau_j)^{m_j}}{\sum_j \left[\frac{\mu}{2} p_{j-1} + \frac{\mu}{2} p_{j+1} + (1-\mu)\, p_j\right]} = \frac{1-\prod_j (1-\tau_j)^{m_j}}{\sum_j p_j} \tag{4}$$

and

$$p_k = 1-(1-\tau_k)^{m_k}. \tag{5}$$

For Ω_1 and Ω_M the terms in p_0 and p_{M+1} should be discarded and the factor $(1-\mu)$ replaced by $(1-\frac{\mu}{2})$.

3. MASTER EQUATION FOR THE LATTICE MODEL

Approximate mean field equations for the lattice model with a single pathogen type can be obtained using simple considerations as follows. The

only accessible variables are the probabilities of finding a susceptible host, x, an infected host, y, and an empty site, $z = 1-x-y$. The rate of increase in the probability of susceptible hosts per generation is assumed proportional to the probability of empty sites z and to the average number of susceptible hosts neighbors to these empty sites. The constant of proportionality is just the birth rate g. The average number of susceptible hosts that are neighbors to an empty site is given by the total number of neighbors to the empty site, ζ, times the probability that a site is occupied by a susceptible host: $\langle n \rangle = \zeta x$. A second contribution to the rate of change in x comes from susceptible hosts becoming infected. This is proportional to x and to the average number of infected neighbors to the susceptible host, $\langle m \rangle = \zeta y$. The constant of proportionality is the transmissibility τ. Therefore,

$$\frac{dx}{dt} = gz\zeta x - \tau x \zeta y. \tag{6}$$

Similarly

$$\frac{dy}{dt} = \tau x \zeta y - vy. \tag{7}$$

These equations can be found in refs. 15 and 16 in the context of the same spatial model and in ref. 18 for a similar spatial predator-prey model. It is immediately clear that these equations fail to take into account the fact that a susceptible cannot be infected twice or that an empty site cannot accommodate more than one offspring (compare with Eq. (1)). These equations are, therefore, only approximations, possibly valid in the limit of small birth and transmissibility rates.

One way to correct the overcounting in the probabilities is to realize that, since $\langle n \rangle = \zeta x$ and $\langle m \rangle = \zeta y$, we may write, according to (1)

$$\frac{dx}{dt} = z[1-(1-g)^{\langle n \rangle}] - x[1-(1-\tau)^{\langle m \rangle}] = z[1-(1-g)^{\zeta x}] - x[1-(1-\tau)^{\zeta y}] \tag{8}$$

and

$$\frac{dy}{dt} = x[1-(1-\tau)^{\langle m \rangle}] - vy = x[1-(1-\tau)^{\zeta y}] - vy. \tag{9}$$

It might seem that this second alternative is better, since it keeps the form of the original transition probabilities. We shall see, however, that this is also incorrect.

In order to find the correct mean field limit of the spatial model, we have to derive the master equation for the probability of the system as a whole. The mean field equations result from approximating all pair (and higher) correlations by simple products of one site averages.[18, 23] We shall follow the presentation of ref. 18, generalizing it to include several types of pathogens.

3.1. Master Equation for Discrete Time Updates

The master equation describes the rate of change in the probability of finding the system in a particular state as a function of time. The master equation is usually presented in differential form, where the time interval between updates is taken to be very small. It is useful, however, to derive first a discrete version of the master equation, avoiding the uncertainties related to the passage from discrete to continuous time.

In order to do so we consider a cellular automaton with asynchronous site updates, where at each time step, only one site, chosen randomly, is updated. In this case the master equation can be written as

$$P(\sigma, t+1) = P(\sigma, t) + \sum_{\sigma'_l} \mathrm{T}(\sigma'_l \to \sigma) - \sum_{\sigma'_r} \mathrm{T}(\sigma \to \sigma'_r), \tag{10}$$

where σ'_l are states that can make a transition to σ by changing only once the state of a single site, i.e., by making a single internal transition, and σ'_r are states to which σ can change by a making single internal transition. $\mathrm{T}(\mu \to \nu)$ is the conditional probability of, being in the state μ, make a transition to the state ν.

To write down the transition probabilities explicitly we need to find the states σ'_l and σ'_r. We start with σ'_l, which we rename as σ^i_k. These states are equal to σ at all sites except at i. At the site i the state is given by

$$\begin{cases} \tau_k & \text{if} \quad \sigma_i = 0 \\ 0 & \text{if} \quad \sigma_i = 1 \\ 1 & \text{if} \quad \sigma_i = \tau_{k'} \qquad \text{for any } k'. \end{cases} \tag{11}$$

σ^i_k can go to σ by a single transition.

We also rename σ'_r as ${}^i\sigma_k$, also defined as equal to σ in all sites except at i. At i the state is given by

$$\begin{cases} 1 & \text{if} \quad \sigma_i = 0 \\ \tau_k & \text{if} \quad \sigma_i = 1 \\ 0 & \text{if} \quad \sigma_i = \tau_{k'} \qquad \text{for any } k'. \end{cases} \tag{12}$$

Note that when $\sigma_i = 0$, the state of σ_k^i at site i may be $\tau_{k'}$ for any k', since all of them can make a transition to 0 with probability $1-(1-g)^n$. Therefore we have to sum over k'. However, if $\sigma_i = \tau_k$, that of σ_k^i at site i is 1. This state may get infected by any $\tau_{k'}$, and we must restrict k' to the original value of the state in σ. Therefore, the index k' in $\sigma_{k'}^i$ must be the same as in σ_i, so that we return exactly to the same state. The result is:

$$P(\sigma, t+1) = P(\sigma, t) + \sum_{i=1}^{N} [T(\sigma_k^i \to \sigma) - T(\sigma \to {}^i\sigma_k)] \tag{13}$$

where, according to Eq. (2),

$$T(\sigma_k^i \to \sigma) = \begin{cases} \sum_{k'} P(\sigma_{k'}^i, t)\, v & \text{if} \quad \sigma_i = 0 \\ P(\sigma_k^i, t)[1-(1-g)^{n_i}] & \text{if} \quad \sigma_i = 1 \\ P(\sigma_k^i, t)\, \Omega_k & \text{if} \quad \sigma_i = \tau_k \end{cases} \tag{14}$$

and

$$T(\sigma \to {}^i\sigma_k) = \begin{cases} P(\sigma, t)[1-(1-g)^{n_i}] & \text{if} \quad \sigma_i = 0 \\ \sum_{k'} P(\sigma, t)\, \Omega_{k'} & \text{if} \quad \sigma_i = 1 \\ P(\sigma, t)\, v & \text{if} \quad \sigma_i = \tau_k. \end{cases} \tag{15}$$

Eq. (13) can be re-written in a simplified form as

$$P(\sigma, t+1) = P(\sigma, t) + \sum_{i=1}^{N} \sum_{k'} [P(\sigma_{k'}^i)\, \omega_{i\sigma_i}(\sigma_{k'}^i) - P(\sigma)\, \omega_{ik'}(\sigma)] \tag{16}$$

remembering that the sum over k' is present only in the cases specified by Eqs. (14) and (15), i.e., when the argument of ω is $\tau_{k'}$ in the first term and when it is 1 in the second term. Eq. (16) is the Master Equation for discrete time updates.

3.2. Master Equation for Continuous Time Updates

In order to derive a continuum master equation for the lattice model, we consider the limit where the interval between updates of the system, δt, becomes infinitesimal. The probability that a site changes its state in this interval becomes likewise small, proportional to δt. However, there is no unique way to assign such infinitesimal change of state from a given discrete update rule. If one considers the simulation process as updates of the *agents*, such as a susceptible host, then in a small time step δt the reproductive rate g becomes proportionally small, $g\,\delta t$. However, if one

considers the simulation process as updates of the *sites*, that might have multiple agents trying to replicate into them, then what becomes infinitesimal is the probability of the site changing itself, i.e., $G \equiv [1-(1-g)^n]$ becomes $G\,\delta t$. The first process considers each agent selected at random and its opportunity to replicate into neighboring cells, allowing this to take place independent of what others are doing. The second process considers all processes that could affect a particular site. The former is not really valid as a model of reality because one cannot ignore what other agents are doing. If an agent replicates into a site, no other neighboring agent can replicate there, no matter how small the replicating probability might be. In other words, the "effective" value of the reproductive rate $g\,\delta t$ must be reduced for an agent by the possibility that other agents make their move before it does. Of course when G becomes small, g becomes small too, since $g = [1-(1-G)^{1/n}]$. This is the strategy behind our continuous time mean field equations. They coincide with those presented in refs. 15 and 16 only in the limit of small reproductive rates and transmissibilities.

Therefore, similarly to Eq. (13), in the limit of small δt, the master equation can be written as

$$\frac{\mathrm{dP}(\sigma, \mathrm{t})}{\mathrm{dt}} = \sum_{\sigma'_l} \mathrm{T}(\sigma'_l \to \sigma) - \sum_{\sigma'_r} \mathrm{T}(\sigma \to \sigma'_r). \tag{17}$$

Using the same reasoning leading to Eq. (16) this can be written as

$$\frac{\mathrm{dP}(\sigma, \mathrm{t})}{\mathrm{dt}} = \sum_{i=1}^{N} \sum_{k'} [P(\sigma^i_{k'})\, \omega_{i\sigma_i}(\sigma^i_{k'}) - P(\sigma)\, \omega_{ik'}(\sigma)]. \tag{18}$$

3.3. Averages of State Functions

Given any function of the states, $f(\sigma)$, its ensemble average at time t is given by

$$\langle f(\sigma) \rangle = \sum_{\sigma} P(\sigma, t)\, f(\sigma). \tag{19}$$

Using the continuous time framework we can differentiate both sides with respect to t and, using the compact notation of (18), we find

$$\begin{aligned} \frac{\mathrm{d}\langle \mathrm{f}(\sigma) \rangle}{\mathrm{dt}} &= \sum_{\sigma} \frac{\mathrm{dP}(\sigma, \mathrm{t})}{\mathrm{dt}} f(\sigma) \\ &= \sum_{i=1}^{N} \left[\sum_{\sigma} \sum_{k'} f(\sigma)\, P(\sigma^i_{k'}, t)\, \omega_{i\sigma_i}(\sigma^i_{k'}) - f(\sigma)\, P(\sigma, t)\, \omega_{ik'}(\sigma) \right]. \end{aligned} \tag{20}$$

Since we are summing over all states, we can replace σ_k^i by σ and σ by ${}^i\sigma_k$ in the first term. We obtain

$$\frac{d\langle f(\sigma)\rangle}{dt} = \sum_{i=1}^{N} \left[\sum_{\sigma} \sum_{k'} f({}^i\sigma_{k'})\, P(\sigma, t)\, \omega_{ik'}(\sigma) - f(\sigma)\, P(\sigma, t)\, \omega_{ik'}(\sigma) \right]$$
$$= \sum_{i=1}^{N} \sum_{k'} \langle [f({}^i\sigma_{k'}) - f(\sigma)]\, \omega_{ik'}(\sigma)\rangle \tag{21}$$

where again the sum over k' exists only when the argument of ω is $\tau_{k'}$ in the first term and when it is 1 in the second term.

In the discrete time scheme the time derivative has to be replaced by the difference between the ensemble averages at times $t+1$ and t. *The condition for stationary averages, therefore, is the same for both cases if we use our version of the continuous time limit.*

4. THE MEAN FIELD APPROXIMATION

In this section and in the remainder of the paper we shall consider only the continuous time limit. The discrete time equations can be obtained by replacing the time derivatives by finite differences of the corresponding quantities. We emphasize that all discrete stationary calculations will be identical to the continuous ones if we use our version of the continuous time limit, although the dynamic approach to equilibrium may be slightly different.

In the case of a single type of pathogen the sum over k' disappears and the transition probabilities simplify to Eq. (1). To obtain an equation for the average probability of, say, empty sites, we consider $f(\sigma) = \delta(\sigma_i, 0)$. Then $P_i(0, t) \equiv \langle \delta(\sigma_i, 0)\rangle$ is the average probability that site i is in the state (0) in the time t. Similarly we define $P_i(1, t)$ for the average probability of susceptible hosts and $P_i(\tau, t)$ for the average probability of infected hosts. In the approximation where the P_i's are independent of the site, they become the mean field probabilities of each state, which we call $x(t) = P(1, t)$, $y(t) = P(\tau, t)$, and $z(t) = P(0, t) = 1 - x(t) - y(t)$.

We start with $f(\sigma) = \delta(\sigma_i, 1)$. According to Eq. (21), we obtain

$$\frac{dP_i(1, t)}{dt} = \sum_{n=1}^{N} \langle f({}^n\sigma)\, \omega_n(\sigma) - f(\sigma)\, \omega_n(\sigma)\rangle. \tag{22}$$

Since $f({}^n\sigma)$ differs from $f(\sigma)$ only if $n = i$, only this term contributes to the sum. Noticing that $\delta({}^i\sigma, 1) = \delta(\sigma_i, 0)$ we get

$$\frac{dP_i(1, t)}{dt} = \langle \delta(\sigma_i, 0)[1 - (1-g)^{n_i}] - \delta(\sigma_i, 1)[1 - (1-\tau)^{m_i}]\rangle. \tag{23}$$

Similarly we obtain

$$\frac{dP_i(\tau, t)}{dt} = \langle \delta(\sigma_i, 1)[1-(1-\tau)^{m_i}] - \delta(\sigma_i, \tau)\, v \rangle. \tag{24}$$

4.1. The Calculation of $\langle \delta(\sigma_i, 0)[1-(1-g)^{n_i}] \rangle$

Expanding the binomial $(1-g)^{n_i}$ we obtain

$$[1-(1-g)^{n_i}] = g n_i + \frac{g^2}{2!} n_i(n_i-1) + \frac{g^3}{3!} n_i(n_i-1)(n_i-2) + \cdots. \tag{25}$$

The number of terms in the series is at most ζ, the total number of neighbors. Using $n_i = \sum_j \delta(\sigma_{i+j}, 1)$ and defining the correlations $P_{ij}(\alpha\beta) = \langle \delta(\sigma_i, \alpha)\, \delta(\sigma_j, \beta) \rangle$, $P_{ijk}(\alpha\beta\gamma) = \langle \delta(\sigma_i, \alpha)\, \delta(\sigma_j, \beta)\, \delta(\sigma_j, \gamma) \rangle$, etc., we find

$$\langle \delta(\sigma_i, 0)[1-(1-g)^{n_i}] \rangle = g \left[\sum_j P_{i, i+j}(01) \right] + \frac{g^2}{2!} \left[\sum_{j \neq k} P_{i, i+j, i+k}(011) \right] + \frac{g^3}{3!} \left[\sum_{j \neq k \neq l} P_{i, i+j, i+k, i+l}(0111) \right] + \cdots. \tag{26}$$

As an illustration we calculate explicitly the term proportional to g^3 in Appendix A. Approximating the correlation of k sites by the product of the corresponding one-site correlations and assuming that these are independent of the site we get

$$\begin{aligned} \langle \delta(\sigma_i, 0)[1-(1-g)^{n_i}] \rangle &\approx g\zeta P(0)\, P(1) + \frac{g^2}{2!} \zeta(\zeta-1)\, P(0)\, P(1)\, P(1) \\ &\quad + \frac{g^3}{3!} \zeta(\zeta-1)(\zeta-2)\, P(0)\, P(1)\, P(1)\, P(1) + \cdots \\ &= \zeta z x + \frac{g^2}{2!} \zeta(\zeta-1)\, z x^2 + \frac{g^3}{3!} \zeta(\zeta-1)(\zeta-2)\, z x^3 + \cdots \\ &= z[1-(1-gx)^{\zeta}]. \end{aligned} \tag{27}$$

Similarly we find

$$\langle \delta(\sigma_i, 1)[1-(1-\tau)^{m_i}] \rangle \approx x[1-(1-\tau y)^{\zeta}]. \tag{28}$$

4.2. Mean Field Equations for one Type of Pathogen

Replacing (27) and (28) into (23) and (24) we obtain

$$\frac{dx}{dt} = zh_\zeta(gx) - xh_\zeta(\tau y) \tag{29}$$

and

$$\frac{dy}{dt} = xh_\zeta(\tau y) - vy \tag{30}$$

where we have defined the auxiliary function

$$h_\zeta(\alpha) \equiv 1-(1-\alpha)^\zeta. \tag{31}$$

These are the correct mean field equations for the host-pathogen model.

It is instructive to study a specific case to understand that Eqs. (29) and (30) are indeed correct. Assume that the number of nearest neighbors is $\zeta = 4$ and that the average density of susceptible hosts is $x = 1/2$. Consider an empty site. Then, the probability of having no nearest neighbor susceptible host to this site is $1/2^4$. That of having 1 nearest neighbor susceptible host is $4/2^4$ and also $6/2^4$, $4/2^4$, $1/2^4$ for 2, 3, and 4 nearest neighbor susceptible hosts respectively. The case of k nearby susceptible hosts contributes a probability $[1-(1-g)^k]$ to the total probability of an offspring in the empty site. Adding them all together we obtain

$$\begin{aligned}\tfrac{1}{2^4}\{&[1-(1-g)^0]+4[1-(1-g)^1]+6[1-(1-g)^2]+4[1-(1-g)^3]\\ &+[1-(1-g)^4]\} = \tfrac{1}{2^4}[4g+6(2g-g^2)+4(3g-3g^2+g^3)\\ &+(4g-6g^2+4g^3-g^4)] = 1-(1-g/2)^4\end{aligned}$$

which is indeed the probability predicted by the first term of (29).

4.3. Comparison with the Approximate Equations

We note that both sets of equations derived by simple hand-waving arguments in Section 3 are wrong, though they can be considered as approximations to the true equations when gx and τy are small. Equations (6) and (7) turn out to be quite accurate for most regions of the $g-\tau$ parameters, whereas (8) and (9) are good only for small gx and τy. The inadequacy of Eqs. (8) and (9) is not surprising, since averaging in the exponent is not a good representation of the average of the actual probability functions over the relevant discrete set of possibilities.

Before showing a direct comparison between simulations obtained from the lattice model and the mean field equations for the host-pathogen model, we illustrate the differences between the exact and approximate equations with a simple "toy" model. This is a useful test, because in this model the mean field is a good approximation over a wide range of parameters. Consider a situation where the lattice sites can be only either empty or occupied by hosts. Hosts can reproduce into neighboring sites with probability g and die at a constant rate μ. The exact mean field equation for the populations of hosts x is

$$\frac{dx}{dt} = (1-x)\, h_\zeta(gx) - \mu x \tag{32}$$

whereas the approximate mean field equation is

$$\frac{dx}{dt} = (1-x)\, \zeta g x - \mu x. \tag{33}$$

Figure 1 shows a comparison between the numerical simulation (with the probabilistic cellular automaton) and the mean field equations. It shows the average population of hosts x at equilibrium as a function of g. The over estimation of the birth rate by the approximate equations is very clear in this case. The accuracy of the exact equations is also very impressive, demonstrating the correctness of our formalism. Note that the discrete time mean field equations we derived would produce results identical to our exact continuous time equations, since Fig. 1 shows the population at equilibrium.

Figure 2 shows the comparison between simulations and mean field equations for the full host-pathogen model for the average populations of susceptible hosts x and infected hosts y. The birth rate is fixed at $g = 0.5$. Panels (a) and (b) compare the lattice simulations with the mean field results for $v = 0.3$ and $v = 0.5$ respectively. For $\tau < 0.5$, the approximate mean field Eqs. (6) and (7) (dotted lines) tend to overestimate the number of infected hosts and underestimate the number of susceptible hosts. The correct mean field, although still not really close to the lattice results, pushes the curves in the right direction. The value of τ where y reaches its maximum, for instance, is about 0.55 for $v = 0.5$, both in the lattice simulation and in the exact mean field calculation. For the approximate mean field, the maximum happens at a much lower value of τ, at $\tau = 0.4$.

Also, the mean field equations are nonlinear, both in the population variables x and y *and* in the parameters g and τ. The nonlinearity in the parameters is responsible for the loss of the scaling invariant transformation

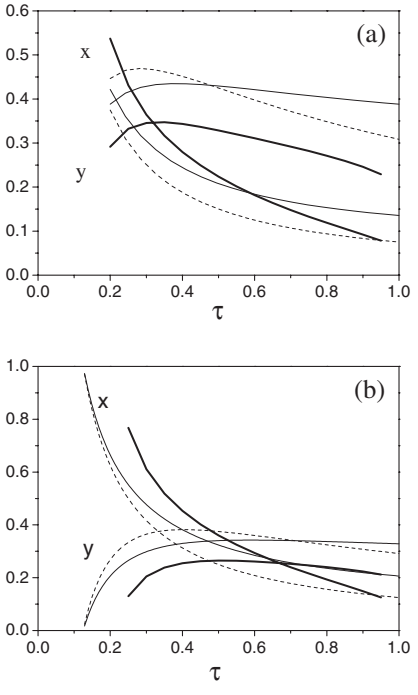

Fig. 2. Comparison between the average populations of susceptible hosts (x) and infected hosts (y) for the lattice simulations (thicker lines) with exact (thick lines) and approximate (dashed lines) mean field calculations. The birth rate is fixed at $g = 0.5$. Panels (a) and (b) compare the lattice simulations with the mean field results for $v = 0.3$ and $v = 0.5$ respectively.

studied in ref. 18. Indeed, for the approximate equations, (6) and (7), it is sufficient to consider $g+\tau+v=1$, whereas these parameters are independent in the spatial model and in the full mean field equations.

We see that the host-pathogen model is less well described by the mean field than the toy model previously discussed. In particular, the number of independent correlations between pairs of sites is larger in the host-pathogen model than in the toy model, indicating that the mean field equations for the former should not be as accurate as for the latter. However, the toy model helps us understand why the approximate mean field equations are nearly as good as the exact equations in the host-pathogen model. The approximate version of Eq. (29) for x overcounts both the reproduction rate of x and their infection rate by y neighbors. These overcountings partialy cancel, resulting in a smaller error than in the simple case discussed above.

4.4. Mean Field Equations for Two Types of Pathogens

Virotic or bacterial infections in real life epidemics are subjected to mutations. A mutant pathogen may have different transmissibility and virulence properties, causing its spread to be more or less effective than that of the resident (original) pathogen. Simulations performed with the spatial model suggest that pathogens types that propagate too fast usually kill all the available susceptible hosts in the neighborhood, causing their own extinction. Considering mutations affecting only the transmissibility leads in some cases to the appearance of an evolutionarily stable type which cannot be invaded by either more or less transmissible mutants. The population of infected individuals stabilizes with a distribution of pathogens centered around the evolutionarily stable type. Can this feature be described within the mean field approximation? The answer, according to the approximate Eqs. (6) and (7), is no. It can be shown that, in this case, a mutant pathogen with transmissibility τ' always invades a resident pathogen with transmissibility τ if $\tau' > \tau$. In this section we show that the true mean field Eqs. (29) and (30) leads to a different result: if $|\tau' - \tau|$ is small, both types of pathogens co-exist in the populations. The average number of infected is $y(\tau') > y(\tau)$ if $\tau' > \tau$.

We shall assume that both the resident and the mutant types have the same virulence v, but different transmissibility rates, τ_1 for the resident and τ_2 for the mutant. There are four one-site variables, z, x, y_1, and y_2, corresponding to the probabilities of empty sites, susceptible hosts, infected by the resident pathogen and infected by the mutant pathogen respectively. Once again $z = 1 - x - y_1 - y_2$.

The complication that arises in the case of more than one type of pathogen is that the transition probability from the state (1) to (τ_1) or (τ_2) becomes even more nonlinear and cumbersome. For the case of two types of pathogens these probabilities are given by (see Section 2)

$$\begin{aligned} P(1 \to \tau_1) &= \chi \left[\frac{\mu}{2} p_2 + \left(1 - \frac{\mu}{2}\right) p_1 \right] \\ P(1 \to \tau_2) &= \chi \left[\frac{\mu}{2} p_1 + \left(1 - \frac{\mu}{2}\right) p_2 \right] \end{aligned} \tag{34}$$

where

$$\chi = \frac{1 - (1-\tau_1)^{m_1} (1-\tau_2)^{m_2}}{2 - (1-\tau_1)^{m_1} - (1-\tau_2)^{m_2}}, \tag{35}$$

and $p_k = 1 - (1-\tau_k)^{\zeta}$. We shall see, nonetheless, that these probabilities can be taken into account exactly.

Using the Master Equation (21), we obtain the following differential equation for x:

$$\frac{\mathrm{dP_i}(1)}{\mathrm{dt}} = \langle \delta(\sigma_i, 0)[1-(1-g)^{n_i}]\rangle - \langle \delta(\sigma_i, 1)[1-(1-\tau_1)^{m_i^1}(1-\tau_2)^{m_i^2}]\rangle \quad (36)$$

where $n_i = \sum_j \delta(\sigma_{i+j}, 1)$ and $m_i^k = \sum_j \delta(\sigma_{i+j}, \tau_k)$ are the number of nearest neighbors to i that are susceptible hosts and infected hosts with pathogen τ_k respectively.

The first term on the right hand side was already calculated in Eq. (27). To calculate the second term one has to expand the two binomials and group terms of the same order in τ_i. After some algebra we find

$$\frac{\mathrm{dx}}{\mathrm{dt}} = z h_\zeta(gx) - x h_\zeta(y_1\tau_1 + y_2\tau_2) \quad (37)$$

The equations for y_1 and y_2 are obtained from

$$\frac{\mathrm{dP_i}(\tau_1)}{\mathrm{dt}} = \left\langle \delta(\sigma_i, 1)\, \chi \left[\frac{\mu}{2} p_2 + \left(1-\frac{\mu}{2}\right) p_1 \right] \right\rangle - \langle \delta(\sigma_i, \tau_1)\, v\rangle \quad (38)$$

and

$$\frac{\mathrm{dP_i}(\tau_2)}{\mathrm{dt}} = \left\langle \delta(\sigma_i, 1)\, \chi \left[\frac{\mu}{2} p_1 + \left(1-\frac{\mu}{2}\right) p_2 \right] \right\rangle - \langle \delta(\sigma_i, \tau_2)\, v\rangle. \quad (39)$$

Instead of deriving the equations for y_1 and y_2 directly, we shall first obtain the equation for $y = y_1 + y_2$, the total number of infected hosts. Adding the two equations above, several simplifications occur. The terms proportional to $\delta(\sigma_i, 1)$ become identical to the second term of Eq. (36) and we obtain

$$\frac{\mathrm{dy}}{\mathrm{dt}} = x h_\zeta(y_1\tau_1 + y_2\tau_2) - vy. \quad (40)$$

Returning to Eqs. (38) and (39) we make the ansatz

$$\langle \delta(\sigma_i, 1)\, \chi p_k\rangle \equiv \chi_k \langle \delta(\sigma_i, 1)\, p_k\rangle, \quad (41)$$

and write

$$\frac{dy_1}{dt} = \chi_2 x \frac{\mu}{2}[1-(1-\tau_2 y_2)^\zeta] + \chi_1 x \left(1-\frac{\mu}{2}\right)[1-(1-\tau_1 y_1)^\zeta] - v y_1 \quad (42)$$

$$\frac{dy_2}{dt} = \chi_1 x \frac{\mu}{2}[1-(1-\tau_1 y_1)^\zeta] + \chi_2 x \left(1-\frac{\mu}{2}\right)[1-(1-\tau_2 y_2)^\zeta] - v y_2. \quad (43)$$

Adding (42) and (43) and comparing with (40) we see that χ_1 and χ_2 must satisfy the relation

$$\chi_1[1-(1-\alpha_1)^\zeta]+\chi_2[1-(1-\alpha_2)^\zeta]=[1-(1-\alpha_1-\alpha_2)^\zeta] \tag{44}$$

where we have defined $\alpha_1 \equiv \tau_1 y_1$ and $\alpha_2 \equiv \tau_2 y_2$ to simplify the notation.

χ_1 and χ_2 are functions of α_1 and α_2. Exchanging α_1 by α_2 does not alter the right-hand-side of (44) and implies that $\chi_2(\alpha_2, \alpha_1) = \chi_1(\alpha_1, \alpha_2)$. Therefore, χ_k can be written in the form

$$\chi_k(\alpha_1, \alpha_2) = \phi(\alpha_1, \alpha_2)\, g(\alpha_k) \tag{45}$$

where $\phi(\alpha_1, \alpha 2) = \phi(\alpha_2, \alpha_1)$ is a symmetric function. We write ϕ as

$$\phi(\alpha_1, \alpha_2) \equiv \frac{[1-(1-\alpha_1-\alpha_2)^\zeta]}{2-(1-\alpha_1)^\zeta-(1-\alpha_2)^\zeta} f(\alpha_1, \alpha_2) \tag{46}$$

where f is another symmetric function. Substituting Eqs. (45) and (46) into (44) and re-arranging the terms we get

$$\begin{aligned}&\{f(\alpha_1, \alpha_2)\, g(\alpha_1)[1-(1-\alpha_1)^\zeta]+(1-\alpha_1)^\zeta\}\\ &\quad+\{f(\alpha_1, \alpha_2)\, g(\alpha_2)[1-(1-\alpha_2)^\zeta]+(1-\alpha_2)^\zeta\}=2.\end{aligned} \tag{47}$$

This equation must hold true for all α_1 and α_2. There are only two possibilities: either each term inside the brackets is equal to 1 or the first term is equal to $1-(1-\alpha_2)^\zeta+(1-\alpha_1)^\zeta$ and the second equal to $1-(1-\alpha_1)^\zeta+(1-\alpha_2)^\zeta$. In appendix B we show that this is indeed true, and that the second choice leads to an inconsistency. This leaves us with the first possibility:

$$\begin{aligned}f(\alpha_1, \alpha_2)\, g(\alpha_1)[1-(1-\alpha_1)^\zeta] &= 1-(1-\alpha_1)^\zeta\\ f(\alpha_1, \alpha_2)\, g(\alpha_2)[1-(1-\alpha_2)^\zeta] &= 1-(1-\alpha_2)^\zeta.\end{aligned} \tag{48}$$

Therefore $f(\alpha_1, \alpha_2)\, g(\alpha_1) = f(\alpha_1, \alpha_2)\, g(\alpha_2) = 1$, $g(\alpha_1) = g(\alpha_2) = constant = c$ and $f(\alpha_1, \alpha_2) = 1/c$. Finally,

$$\begin{aligned}\chi_1 = \chi_2 \equiv \bar{\chi} &= \frac{1-(1-\tau_1 y_1-\tau_2 y_2)^\zeta}{2-(1-\tau_1 y_1)^\zeta-(1-\tau_2 y_2)^\zeta}\\ &= \frac{h_\zeta(\tau_1 y_1+\tau_2 y_2)}{h_\zeta(\tau_1 y_1)+h_\zeta(\tau_2 y_2)}\end{aligned} \tag{49}$$

and Eqs. (42) and (43) become

$$\frac{dy_1}{dt} = \bar{\chi} x \left\{ \frac{\mu}{2} h_\zeta(\tau_2 y_2) + \left(1 - \frac{\mu}{2}\right) h_\zeta(\tau_1 y_1) \right\} - v y_1 \tag{50}$$

$$\frac{dy_2}{dt} = \bar{\chi} x \left\{ \frac{\mu}{2} h_\zeta(\tau_1 y_1) + \left(1 - \frac{\mu}{2}\right) h_\zeta(\tau_2 y_2) \right\} - v y_2. \tag{51}$$

4.5. Invasion and Co-Existence

Setting the mutation rate to zero, Eqs. (50) and (51) become

$$\frac{\mathrm{dx}}{\mathrm{dt}} = z h_\zeta(gx) - x h_\zeta(\tau_1 y_1 + \tau_2 y_2) \tag{52}$$

$$\frac{dy_1}{dt} = \bar{\chi} x h_\zeta(\tau_1 y_1) - v y_1 \tag{53}$$

$$\frac{dy_2}{dt} = \bar{\chi} x h_\zeta(\tau_2 y_2) - v y_2. \tag{54}$$

The approximate equations, valid if $\tau_1 y_1$, $\tau_2 y_2$, and gx are much smaller than one, are simply

$$\frac{dx}{dt} = g\,\zeta z x - \zeta x(\tau_1 y_1 + \tau_2 y_2) \tag{55}$$

$$\frac{dy_1}{dt} = \zeta x \tau_1 y_1 - v y_1 \tag{56}$$

$$\frac{dy_2}{dt} = \zeta x \tau_2 y_2 - v y_2. \tag{57}$$

Setting $\dot{x} = \dot{y}_1 = \dot{y}_2 = 0$ we get the equilibrium solutions. For the case of the approximate equations there are only two possibilities for $\tau_2 \neq \tau_1$:

$$\begin{aligned} y_1 &= 0 \qquad y_2 = \frac{g}{\zeta \tau_2} \frac{\zeta \tau_2 - v}{\tau_2 + g} \qquad x = \frac{v}{\zeta \tau_2} \\ y_2 &= 0 \qquad y_1 = \frac{g}{\zeta \tau_1} \frac{\zeta \tau_1 - v}{\tau_1 + g} \qquad x = \frac{v}{\zeta \tau_1} \end{aligned} \tag{58}$$

No co-existence is possible, unless $\tau_1 = \tau_2$.

Unfortunately, it is not possible to solve our mean field equations analytically to find the stationary solutions. However, we can solve them approximately: instead of setting $1-(1-\tau_i y_i)^\zeta \approx \zeta\tau_i y_i$, we go one step further and make $1-(1-\tau_i y_i)^\zeta \approx \zeta\tau_i y_i[1-(\zeta-1)\,\tau_i y_i/2]$. In this approximation, Eqs. (53) and (54) with $\dot{y}_1 = \dot{y}_2 = 0$ lead to

$$\bar{\chi} x\, \zeta\tau_1[1-(\zeta-1)\,\tau_1 y_1/2] = v \tag{59}$$

$$\bar{\chi} x\, \zeta\tau_2[1-(\zeta-1)\,\tau_2 y_2/2] = v. \tag{60}$$

Dividing one equation by the other and re-arranging the terms we get

$$y_2 = 2\,\frac{\tau_2-\tau_1}{(\zeta-1)\,\tau_2^2} + y_1\left(\frac{\tau_1}{\tau_2}\right)^2. \tag{61}$$

If $\tau_2 = \tau_1$ we get $y_2 = y_1$. However, both y_1 and y_2 can be non-zero simultaneously. This implies co-existence, a feature that cannot be obtained with the approximate equations. It appears only when the probabilities of infection are correctly calculated. These probabilities are smaller than those predicted by the approximate mean field equations. When a small amount of the mutant pathogen is introduced, it does not spread as effectively as one would expect, making co-existence possible. The overcount of the probabilities in the approximate equations rules out this possibility.

From a mathematical point of view, the equilibrium conditions for Eqs. (56) and (57) form a homogeneous linear system in y_1 and y_2, and the non-trivial solution requires $\tau_1 = \tau_2$. The nonlinear terms in Eqs. (53) and (54), that correct the overcounting, make the non-trivial solution possible for $\tau_2 \neq \tau_1$. Since the correction terms are usually small, we expect co-existence only if $\tau_2 - \tau_1$ is small. And indeed, the numerical simulations show co-existence only for $\Delta \equiv \tau_2 - \tau_1$ small. Expanding Eq. (61) to first order in Δ gives

$$y_2 \approx y_1 + \frac{2\Delta}{\tau_1}\left(\frac{1}{(\zeta-1)\,\tau_1} - y_1\right) \approx y_1 + \frac{2\Delta}{3\tau_1^2} \tag{62}$$

where we have used $\zeta = 4$ and discarded y_1 with respect to $1/3\tau_1$ (typically y_1 is small). For τ_2 close to τ_1, the total number of infected $y = y_1 + y_2$ is given approximately by

$$y \approx \frac{g}{4\tau_1}\,\frac{4\tau_1 - v}{\tau_1 + g}. \tag{63}$$

When $y_2 = y$, and $y_1 = 0$, we get invasion (the trivial solution). This gives

$$\Delta_0 \approx \frac{3g\tau_1}{8}\,\frac{4\tau_1 - v}{\tau_1 + g}. \tag{64}$$

If $\Delta < \Delta_0$ we expect co-existence, otherwise invasion.

Invasion can also be studied with linear stability analysis. Assuming an initial population at equilibrium, with x_0 susceptible hosts and y_{10} infected by the resident pathogen, with transmissibility τ_1, a small amount of a second pathogen, with transmissibility τ_2, is introduced. If the mutation rate is set to zero, the growth rate of the new type is given by

$$\lambda = \frac{d}{dy_2}\{\bar{\chi}x\,[1-(1-\tau_2 y_2)^{\zeta}] - vy_2\}|_{y_2=0} = \zeta x_0 \tau_2 - v. \tag{65}$$

For the approximate mean field equations, $x_0 = v/\zeta\tau_1$ and $\lambda = v(\tau_2 - \tau_1)/\tau_1$. This implies that the probability of any pathogen type with a larger transmissibility than the resident type increases exponentially with time, leading to invasion. For the full mean field equations, however, that is not true, since $x_0 \neq v/\zeta\tau_1$. The numerical integration of the equations of motion reveals that indeed there is no invasion if τ_2 is slightly larger than τ_1. Also if τ_2 is slightly smaller than τ_1 co-existence also occurs.

Figure 3 shows an example for $g = 0.05$, $v = 0.2$ and $\tau_1 = 0.4$. We show the time evolution of the populations starting from $x_0 = 0.125$, $y_{10} = 0.097$ and $y_{20} = 0.001$. Panel (a) shows y_1 versus y_2 and panel (b) x versus y_2 for $\tau_2 = 0.39$. The approximate equations lead to the extinction of y_2, whereas the correct mean field equations result in co-existence of the two pathogens, y_1 being larger than y_2. Panels (c) and (d) show y_1 versus y_2 and x versus y_1 respectively for $\tau_2 = 0.41$. Again, the approximate equations lead to the extinction of y_1, whereas the correct mean field equations result in co-existence, this time with $y_2 > y_1$. For these values of the parameters, Eq. (64) gives $\Delta_0 = 0.023$, against a numerically calculated threshold, using the full mean field equations, of 0.025.

5. THE PAIR APPROXIMATION FOR A SINGLE PATHOGEN TYPE

The mean field equations can be improved by including pair correlations. This is done by keeping two-site probabilites $P_{ij}(\alpha\beta)$ in the equations while reducing higher order correlations to at most two-site terms. We do this reduction according to the truncation scheme in refs. 18 and 24–26.

Consider a cluster C of $n+1$ sites consisting of the reference site i plus a surrounding cluster R of n neighbors, $n \leqslant \zeta$. The probability of such a cluster, $\mathscr{P}(C)$, can be approximated by a composition of probabilities of subclusters of size 2. We first write $\mathscr{P}(C) = \mathscr{P}(i)\,\mathscr{P}(R \mid i)$. Then, the conditional probability $\mathscr{P}(R \mid i)$ is approximated by the product $\Pi_{j \in R}\,\mathscr{P}(j \mid i)$, where j labels single sites in R:

$$\mathscr{P}(C) = \mathscr{P}(i)\,\mathscr{P}(R \mid i) \approx \mathscr{P}(i) \prod_{j \in R} \mathscr{P}(j \mid i) = \mathscr{P}(i) \prod_{j \in R} \frac{\mathscr{P}(ji)}{\mathscr{P}(i)} \tag{66}$$

where $\mathscr{P}(ji)$ is the probability of the pair (ij).

5.1. Dynamic Equations

For the three possible states per site, (0), (1), and (τ), there are six two-site correlations. Since $\sum_j P(ij) = P(i)$, only three of them are independent. We call the independent correlations $u = P(10)$, $r = P(1\tau)$, and $w = P(0\tau)$. The other three are given by $q \equiv P(00) = z - u - w$, $p \equiv P(11) = x - r - u$, and $s \equiv P(\tau\tau) = y - r - w$, with $z = 1 - x - y$. The five independent variables are, therefore, x, y, u, r, and w.

To write down the equation for x in the pair approximation, we follow the steps leading to Eqs. (23), (25), and (26). The reference site in Eq. (26) is $\sigma_i = (0)$. According to (66), the term $\sum_{j \neq k \neq l} P_{i, i+j, i+k, i+l}(0111)$, for instance, is approximated by

$$\sum_{j \neq k \neq l} P_{i, i+j, i+k, i+l}(0111) \approx \zeta(\zeta-1)(\zeta-2)\,\frac{P(10)\,P(10)\,P(10)}{P(0)\,P(0)}. \tag{67}$$

The analogue of the mean field average, Eq. (27), is, therefore,

$$\begin{aligned}
&\langle \delta(\sigma_i, 0)[1-(1-g)^{n_i}] \rangle \\
&\quad \approx g\zeta P(01) + \frac{g^2}{2!}\,\zeta(\zeta-1)\,\frac{P(10)\,P(10)}{P(0)} \\
&\qquad + \frac{g^3}{3!}\,\zeta(\zeta-1)(\zeta-2)\,\frac{P(10)\,P(10)\,P(10)}{P(0)\,P(0)} + \cdots \\
&\quad = \zeta u/z + \frac{g^2}{2!}\,\zeta(\zeta-1)\,u^2/z + \frac{g^3}{3!}\,\zeta(\zeta-1)(\zeta-2)\,u^3/z + \cdots \\
&\quad = z[1-(1-gu/z)^{\zeta}].
\end{aligned} \tag{68}$$

After a similar manipulation of the term involving τ we find

$$\frac{dx}{dt} = zh_\zeta(gu/z) - xh_\zeta(\tau r/x) \tag{69}$$

and

$$\frac{dy}{dt} = xh_\zeta(\tau r/x)^\zeta - vy. \tag{70}$$

The equations for u, r, and w can be obtained in a similar fashion. The result is

$$\frac{du}{dt} = (q-u)\, h_{\zeta-1}(gu/z) + vr - uh_{\zeta-1}(\tau r/x) - gu[1 - h_{\zeta-1}(gu/z)] \tag{71}$$

$$\frac{dr}{dt} = (p-r)\, h_{\zeta-1}(\tau r/x) - vr - w\, h_{\zeta-1}(gu/z) - \tau r[1 - h_{\zeta-1}(\tau r/x)] \tag{72}$$

$$\frac{dw}{dt} = uh_{\zeta-1}(\tau r/x) + v(s-w) - w\, h_{\zeta-1}(gu/z). \tag{73}$$

5.2. Comparison with the Approximate Equations

Similar to what happens in the mean field limit, Eqs. (69)–(73) reduce to those in ref. 18 in the limit of small gu/z and $\tau r/x$. Perhaps the most striking qualitative difference between our equations and the approximate set in ref. 18 is the existence of limit cycle solutions in the latter for a much larger range of parameters than in the former. An exploration of the parameter space indicates limit cycles occur only for very small virulences and also small g and τ.

Figure 4 shows examples of the different behaviors obtained from the exact and approximate equations. We have fixed $v = 0.1$ and initial conditions $x(0) = y(0) = 0.25$, $u(0) = r(0) = w(0) = 0.1$. The panels show the time evolution of the number of susceptible, x, versus the number of infected, y, for (a) $g = \tau = 0.2$; (b) $g = \tau = 0.4$; (c) $g = \tau = 0.6$; and (d) $g = \tau = 0.8$. In Fig. 4a both curves are stable focuses. As g and τ increase, in Fig. 4b, the differences start to become apparent. In Fig. 4c both curves are still focuses, but the approximate curve oscillates much faster than the exact one. Finally, in Fig. 4d the approximate curve is a limit cycle, whereas the exact is still a focus. Notice that the amplitude of oscillations in the limit cycle is quite large, about 0.3 in the infected and 0.15 in the susceptible densities.

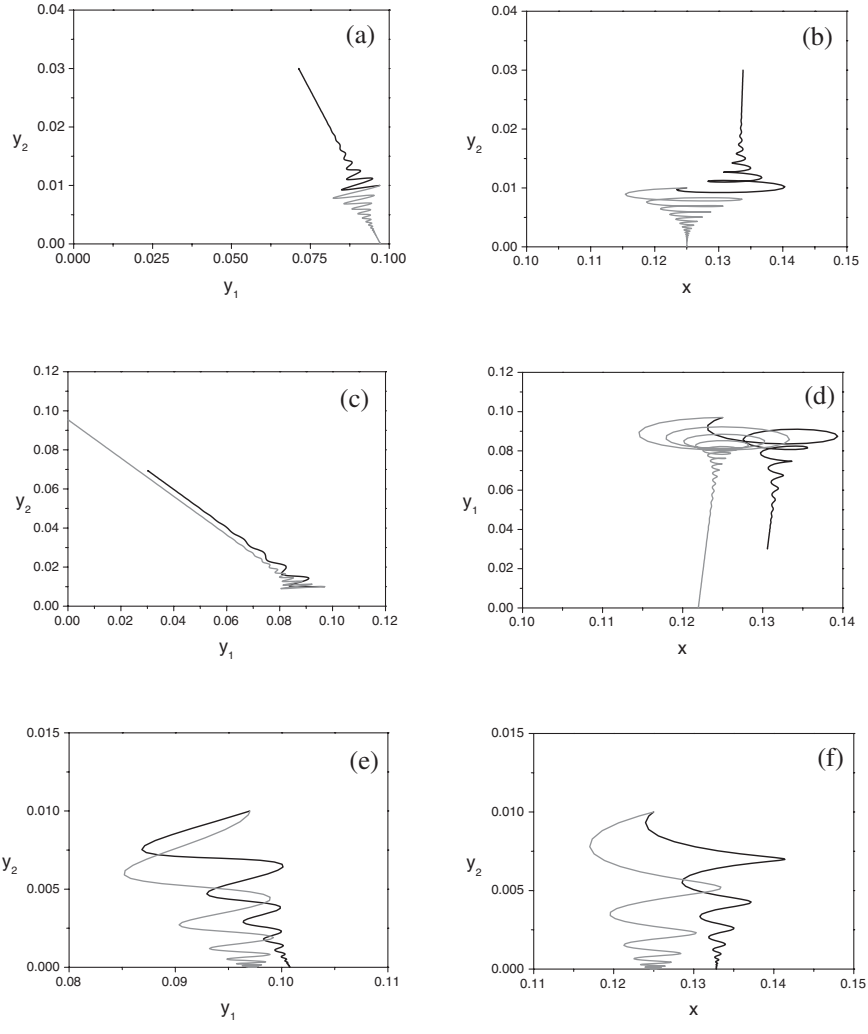

Fig. 3. Co-existence and invasion in the mean field approximations. Thick lines correspond to the full mean field equations and thin lines to the approximate equations. Panels (a) and (b) show the co-existence of the invading and resident pathogens in the case $\tau_1 = 0.4$ (resident) and $\tau_2 = 0.39$ (invading). Part (a) shows y_2 versus y_1 and (b) y_2 versus x. Panels (c) and (d) show similar plots for $\tau_2 = 0.41$. The approximate equations lead to the complete dominance of the more transmissible type. Panels (e) and (f) are similar to (a) and (b), but with $\tau_2 = 0.35$. In this case the more transmissible type dominates over the less transmissible in both the approximate and full mean field equations.

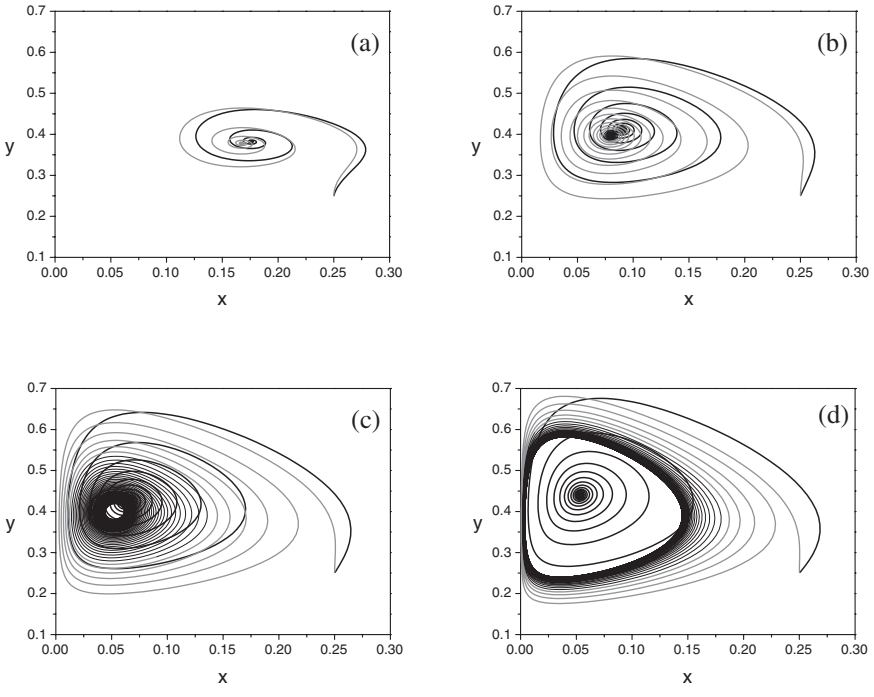

Fig. 4. Comparison between exact mean field including pair correlations (thick lines) and approximate mean field with pair correlations (thin lines). Panels (a) to (d) show the time evolution of the number of susceptibles, x, versus the number of infected, y, for $v = 0.1$ and (a) $g = \tau = 0.2$; (b) $g = \tau = 0.4$; (c) $g = \tau = 0.6$; and (d) $g = \tau = 0.8$. The initial conditions for all panels are $x(0) = y(0) = 0.25$, $u(0) = r(0) = w(0) = 0.1$.

We remark that the spatial model in ref. 18 does show limit cycle oscillations in accordance with the predictions of the approximate equations. However, that model is different from ours and from that in ref. 13 exactly because it overcounts the probabilities of infection and of birth, as discussed earlier.

Figure 5 shows the same lattice simulations displayed in Fig. 2, this time compared against the mean field equations including pair correlations, both exact and approximate. The inclusion of pair correlations represents a great improvement with respect to the bare mean field and the differences between exact and approximate equations become less important. The approximate results still tend to overestimate slightly the number of infected hosts. For $v = 0.3$, the agreement between the lattice and exact mean field calculations for the number of susceptible hosts (panel a) is extremely good. Surprisingly, the approximated mean field gives better

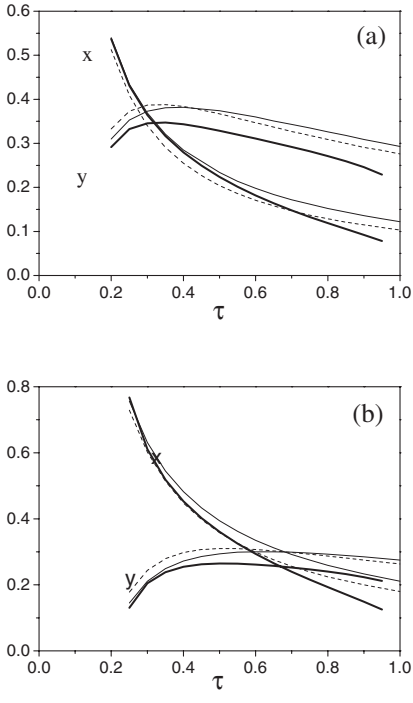

Fig. 5. Comparison between the average populations of susceptible hosts (x) and infected hosts (y) for the lattice simulations (thicker lines) with the exact (thick lines) and approximate (dashed lines) mean field calculations including pair correlations. The birth rate is $g = 0.5$ and the virulence is $v = 0.3$ in panel (a) and $v = 0.5$ in panel (b).

results for $v = 0.5$ (panel b). In any case, we do not expect the mean field results to reproduce exactly the lattice calculations. Further improvement would require the inclusion of higher order correlations.

6. THE DYNAMICS OF INVASION IN THE PAIR APPROXIMATION

In this section we go back to the problem of invasion of an endemic population by a mutant pathogen of different transmissibility. In the spatial version of the model it is known that the system may evolve spontaneously towards an evolutionarily stable pathogen type that cannot be invaded even by more transmissible ones.[4] The basic reason for the appearance of this evolutionarily stable type of intermediate transmissibility lies in the self-organized spatial structure of the population. Hosts and pathogens are distributed patchily. Mutant pathogens can arise that spread more quickly than susceptible hosts are replenished, but these

pathogens cause the extinction of the host and themselves only locally. Can the dynamics in the pair approximation account for this spatial phenomenon?

In order to investigate this possibility we assume once again that both the resident and the mutant pathogens have the same virulence v, but different transmissibility rates: τ_1 for the resident and τ_2 for the mutant. There are four one-site variables, z, x, y_1 and y_2, and 10 two-site variables: $u = P(10)$, $r_1 = P(1\tau_1)$, $r_2 = P(1\tau_2)$, $w_1 = P(0\tau_1)$, $w_2 = P(0\tau_2)$, $q = P(00)$, $p = P(1q)$, $s_1 = P(\tau_1\tau_1)$, $s_2 = P(\tau_2\tau_2)$, and $s_{12} = P(\tau_1\tau_2)$. Of these fourteen variables, only nine are independent. We choose them to be x, y_1, y_2, u, r_1, r_2, w_1, w_2, and s_{12}. The other five are related to them by

$$\begin{aligned} q &= z - u - w_1 - w_2 \\ p &= x - u - r_1 - r_2 \\ s_1 &= y_1 - w_1 - r_1 - s_{12} \\ s_2 &= y_2 - w_2 - r_2 - s_{12} \end{aligned} \tag{74}$$

Using the same type of considerations presented in Section 4.3 we obtain the following set of differential equations:

$$\frac{dx}{dt} = z h_\zeta(gu/z) - x h_\zeta((\tau_1 r_1 + \tau_2 r_2)/x)$$

$$\frac{dy_1}{dt} = \bar{\chi} x \left\{ \frac{\mu}{2} h_\zeta(\tau_2 r_2/x) + \left(1 - \frac{\mu}{2}\right) h_\zeta(\tau_1 r_1/x) \right\} - v y_1$$

$$\begin{aligned} \frac{du}{dt} = {} & (q-u)\, h_{\zeta-1}(gu/z) - gu[1 - h_{\zeta-1}(gu/z)] \\ & - u h_{\zeta-1}((\tau_1 r_1 + \tau_2 r_2)/x) + v(r_1 + r_2) \end{aligned}$$

$$\begin{aligned} \frac{dr_1}{dt} = {} & \bar{\bar{\chi}} \frac{\mu}{2} p h_{\zeta-1}(\tau_2 r_2/x) + \bar{\bar{\chi}} \left(1 - \frac{\mu}{2}\right) p h_{\zeta-1}(\tau_1 r_1/x) \\ & - w_1\, h_{\zeta-1}(gu/z) - \tau_1 r_1 [1 - h_{\zeta-1}((\tau_1 r_1 + \tau_2 r_2)/x)] \\ & - r_1\, h_{\zeta-1}((\tau_1 r_1 + \tau_2 r_2)/x)) - v r_1 \end{aligned}$$

$$\begin{aligned} \frac{dw_1}{dt} = {} & \bar{\bar{\chi}} \frac{\mu}{2} u h_{\zeta-1}(\tau_2 r_2/x) + \bar{\bar{\chi}} \left(1 - \frac{\mu}{2}\right) u h_{\zeta-1}(\tau_1 r_1/x) \\ & + v(s_1 + s_{12} - w_1) - w_1\, h_{\zeta-1}(gu/z) \end{aligned}$$

$$\frac{ds_{12}}{dt} = \bar{\bar{\chi}}\frac{\mu}{2} r_2\{\tau_2[1-h_{\zeta-1}(\tau_2 r_2/x)]+h_{\zeta-1}(\tau_2 r_2/x)\}$$

$$+\bar{\bar{\chi}}\frac{\mu}{2} r_1\{\tau_1[1-h_{\zeta-1}(\tau_1 r_1/x)]+h_{\zeta-1}(\tau_1 r_1/x)\}$$

$$+\bar{\bar{\chi}}\left(1-\frac{\mu}{2}\right) r_2\, h_{\zeta-1}(\tau_1 r_1/x)$$

$$+\bar{\bar{\chi}}\left(1-\frac{\mu}{2}\right) r_1\, h_{\zeta-1}(\tau_2 r_2/x) - 2v s_{12}$$

where

$$\bar{\bar{\chi}} \equiv \frac{h_{\zeta-1}(\tau_1 y_1+\tau_2 y_2)}{h_{\zeta-1}(\tau_1 y_1)+h_{\zeta-1}(\tau_2 y_2)}.$$

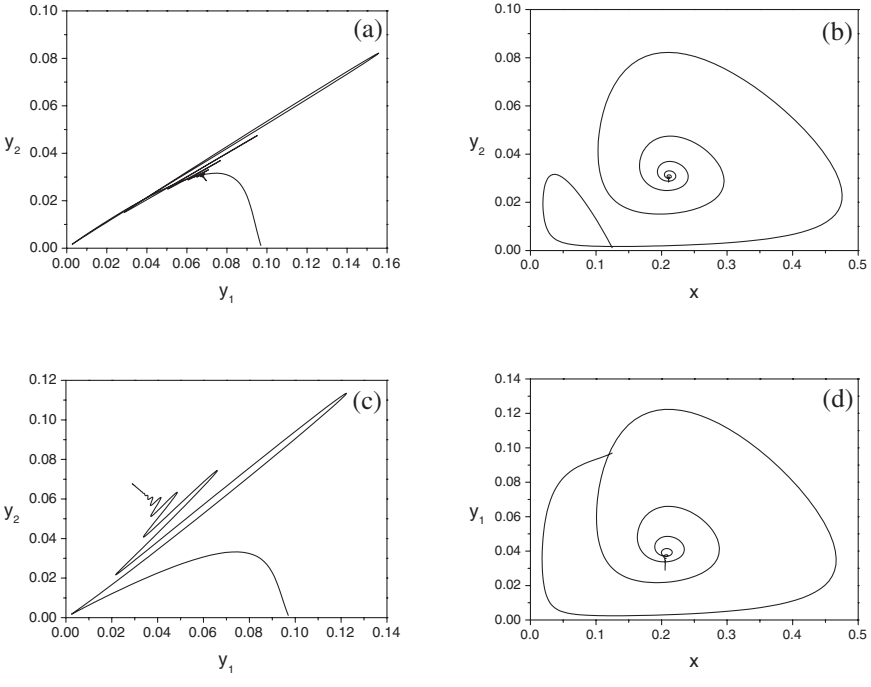

Fig. 6. Co-existence in the pair approximation. The initial populations are $x_0 = 0.125$, $y_{10} = 0.097$, and $y_{20} = 0.001$. Panels (a) and (b) show the process of invasion of a resident pathogen with $\tau_1 = 0.4$ by a small amount of a less transmissible pathogen with $\tau_2 = 0.39$. Part (a) shows y_2 versus y_1 and (b) y_2 versus x. Panels (c) and (d) show similar plots for the case $\tau_2 = 0.41$. The final state shows co-existence in both cases.

The equations for y_2, r_2 and w_2 can be obtained by exchanging the sub-indexes 1 and 2 in the equations for y_1, r_1, and w_1 respectively.

Figure 6 shows the time evolution of x, y_1 and y_2 for the same parameters as in Fig. 3, i.e., $g = 0.05$, $v = 0.2$, and $\tau_1 = 0.4$. The initial conditions are $x_0 = 0.125$, $y_{10} = 0.097$, and $y_{20} = 0.001$. Panels (a) and (b) show y_1 versus y_2 and x versus y_2 respectively for $\tau_2 = 0.39$. Panels (c) and (d) show y_1 versus y_2 and x versus y_1 for $\tau_2 = 0.41$. Comparing these results with those in Fig. 3, we see that the final equilibrium state of the populations is very similar. In particular, the co-existence of the two types of pathogen persists in the pair approximation. The main difference is the approach to equilibrium: the stable node type of approach in Figs. 3b and 3d is replaced by a stable focus in Figs. 6b and 6d, promoting oscillations of quite large amplitudes. Also, the equilibrium value of x changes considerably, going from about 0.13 in the mean field approximation to about 0.21 in the pair approximation.

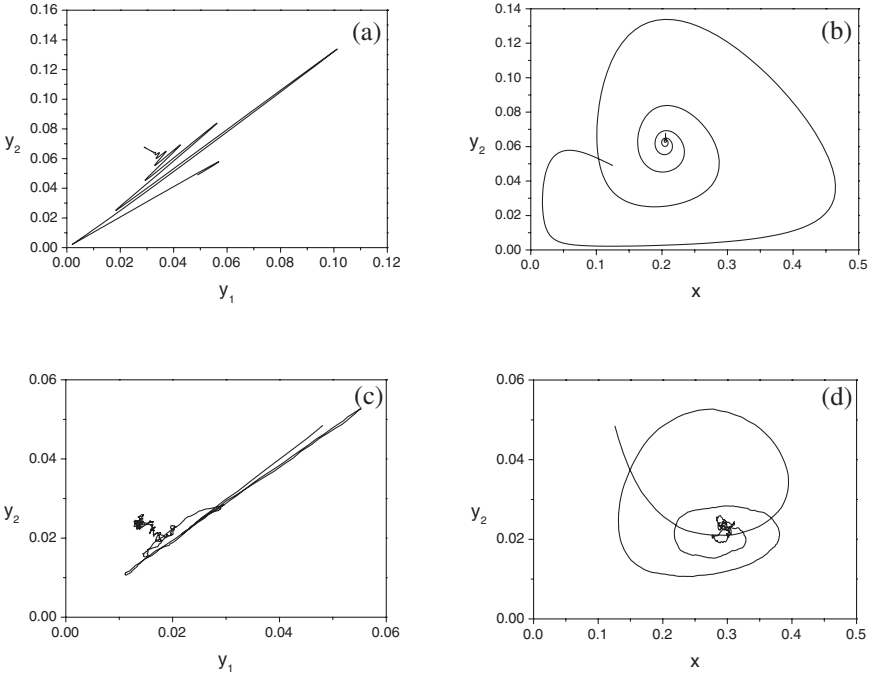

Fig. 7. Pair approximation versus lattice model. The initial population has equal amounts of infected hosts: $x_0 = 0.125$, $y_{10} = y_{02} = 0.049$, $\tau_1 = 0.4$, and $\tau_2 = 0.41$ Parts (a) and (b) show y_2 versus y_1 and y_2 versus x for the pair approximation. Panels (c) and (d) show the same quantities computed with the lattice model.

Figure 7 shows a comparison with the lattice model. The parameters are the same as in Figs. 5c and 5d, but y_1 and y_2 start off with equal amounts: $y_{10} = y_{20} = 0.049$. The qualitative resemblance between the pair approximation, panels (a) and (b), and the lattice calculations, panels (c) and (d), is very good. The number of infected individuals, however, is almost three times smaller in the lattice calculation. Also, the population of y_1 eventually die in the lattice model, although it takes about 8000 generations.

7. DISCUSSION AND CONCLUSIONS

In this work we presented a derivation of mean field equations of a well known host-pathogen model, taking fully into account the fact that a susceptible host cannot become infected twice and that an empty site can accommodate only one offspring. In the context of predator-prey models this limitation implies that a prey cannot be eaten twice by predators. The consequences of including this feature, usually present in spatial models (see however ref. 18), in the mean field equations, are of both qualitative and quantitative natures. On the qualitative side, the equations become nonlinear in g and τ, losing the scaling invariance that allows one to consider only $g+\tau+v=1$.[18] The latter approximation is valid only for small g and τ, where the chances of a susceptible host being infected twice can be neglected. The approximate equations lead to complete invasion if a small amount of a more transmissible mutant pathogen is introduced in the resident population, whereas the full mean field equations lead to co-existence if $|\tau_2-\tau_1|$ is sufficiently small. Invasion happens only if $|\tau_2-\tau_1|$ is larger than a threshold that depends on τ_1.

When pair correlations are taken into account, we found that the approximate equations present limit cycles in a much larger range of parameters than the true mean field equations. Once again, when the process of invasion is studied (see Fig. 6), we find co-existence of similar types if $|\tau_2-\tau_1|$ is small. However, the more transmissible pathogen type still wins over any less transmissible ones, in the sense that either the less transmissible type goes extinct, or its average number is always smaller than the mutant invader. The emergence of an intermediate-transmissibility evolutionarily stable type is not observed even in the pair approximation. This result requires either higher order correlations or more direct representation of the spatial structure of the system. Numerical simulations of the spatial model show that high-transmissibility types go extinct only locally, due to the patchiness of the population. They cause the extinction of hosts available to them in a local patch, thus causing their own extinction, but not that of other types. Patchiness is essential, since this prevents

the spreading of the pathogen to the rest of the population before its death. In a continuous model, even with pair correlations, patches cannot be taken into account, and the more transmissible type ends up wining over the less transmissible.

However, the oscillatory approach to equilibrium revealed by the pair approximation does give us a clue to understand how the evolutionarily stable type appears in the spatial model. In Fig. 8 we show y_1 versus y_2 for $g = 0.05$, $v = 0.2$, and $\tau_2 = \tau_1 + 0.05$ for $\tau_1 = 0.2$, 0.3, and 0.5. Although invasion occurs in all cases, the higher the value of τ_1, the closer the population of infected hosts gets to extinction. Denote by t_c the time when this near-extinction occurs. If we assume that the initial equilibrium population, infected by the resident pathogen alone, is structured in patches, those patches receiving the mutant type are indeed likely to go extinct at $t = t_c$. If the patches are very large, Fig. 8 shows that the number of infected rises again after t_c leading to invasion by the more transmissible type. However, if the patches are finite, the population of infected may die. We can estimate the minimum size of these patches so that extinction can be prevented. If n_p is the total number of sites in the patch and $y_{1\,\min}$, $y_{2\,\min}$ are the values assumed by y_1 and y_2 at $t = t_c$, then the actual number of individuals (sites) infected by the resident and the mutant pathogen types at t_c is $n_p\, y_{1\,\min}$ and $n_p\, y_{2\,\min}$ respectively. When this number goes below 1 there is less than one infected site in the whole patch, and the corresponding pathogen goes extinct. For $\tau_1 = 0.2$ the resident type disappears if n_p is less than 100, whereas the mutant type disappears only if the patch falls below 45

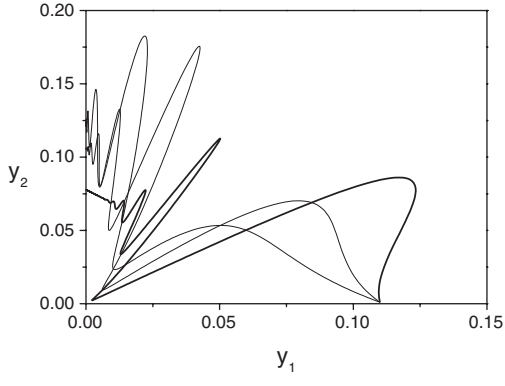

Fig. 8. Invasion in the pair approximation for $g = 0.05$, $v = 0.2$, and $\tau_2 = \tau + 0.05$. The curves show the time evolution for $\tau_1 = 0.2$ (thin), 0.3 (thicker), and 0.5 (thickest). The initial conditions are $x = 0.28$, $y_1 = 0.11$, and $y_2 = 0.001$. The larger the value of τ_1, the closer to extinction the population gets.

sites. Typical patches observed in numerical simulations are larger than this, implying that invasion is indeed expected. For $\tau_1 = 0.5$ extinction of both resident and mutant pathogens is prevented only if patches are larger than about 450. However, for $\tau_1 = 0.7$, the mutant pathogen with $\tau_2 = 0.75$, is more likely to go extinct than the resident. If patches are larger than about 780 the resident pathogen survives, whereas the mutant type disappears unless patches are larger than 890.

In summary, spatial structure is essential for the emergence of an evolutionarily stable pathogen. In the spatial model, the populations organize themselves spontaneously into dynamical patches. The mean field approximation is a limit of infinitely large populations, where patches do not form. In this limit, even including pair correlations, any small amount of a more rapidly transmitting pathogen lead to its invasion over the resident type. However, for large transmissibilities, invasion occurs through a process that leads first to 'near-extinction'. If the actual size of the system, or patch where the mutant first appear, is sufficiently small, extinction does happen for pathogens of large transmissibility, stopping invasion and leading naturally to the survival of an intermediate type.

APPENDIX A: CALCULATION OF THE MEAN FIELD EQUATIONS

In this appendix we illustrate the calculation of the mean field limit by computing terms proportional to g^3 in Eqs. (23)–(25). Explicitly, we calculate

$$\langle \delta(\sigma_i, 0)\, n_i(n_i-1)(n_i-2)\rangle = \langle \delta(\sigma_i, 0)(n_i^3 - 3n_i^2 + 2n_i)\rangle \tag{A1}$$

where $n_i = \sum_j \delta(\sigma_{i+j}, 1)$ is the number of susceptible hosts that are nearest neighbors of i. The first term on the right side, proportional to n_i^3, is

$$\begin{aligned}
&\sum_{j,k,l} \langle \delta(\sigma_i, 0)\, \delta(\sigma_{i+j}, 1)\, \delta(\sigma_{i+k}, 1)\, \delta(\sigma_{i+l}, 1)\rangle \\
&\quad = \sum_{j\neq k\neq l} \langle \delta(\sigma_i, 0)\, \delta(\sigma_{i+j}, 1)\, \delta(\sigma_{i+k}, 1)\, \delta(\sigma_{i+l}, 1)\rangle \\
&\qquad + \sum_{j\neq k} 3\langle \delta(\sigma_i, 0)\, \delta(\sigma_{i+j}, 1)\, \delta(\sigma_{i+k}, 1)\rangle \\
&\qquad + \sum_{j} \langle \delta(\sigma_i, 0)\, \delta(\sigma_{i+j}, 1)\rangle.
\end{aligned} \tag{A2}$$

The right hand side of this equation has three contributions. The first accounts for the cases where all three susceptible neighbors occupy a different site. If two of the j, k, l indices are the same, then there are only two susceptible neighbors. The factor 3 takes care of the three possibilities in which this might happen: $j = k$, $k = l$, and $j = l$. The last term accounts for the case where all three indices are the same. In terms of cluster probabilities we have

$$\begin{aligned}\langle \delta(\sigma_i, 0)\, n_i^3 \rangle &= \sum_{j\neq k\neq l} P_{i,i+j,i+k,i+l}(0111) + \sum_{j\neq k} 3P_{i,i+j,i+k}(011) + \sum_j P_{i,i+j}(01) \\ &= \zeta(\zeta-1)(\zeta-2)\, P(0111) + 3\zeta(\zeta-1)\, P(011) + \zeta P(01) \\ &= \zeta(\zeta-1)(\zeta-2)\, P(0)\, P(1)^3 + 3\zeta(\zeta-1)\, P(0)\, P(1)^2 + \zeta P(0)\, P(1) \\ &= \zeta(\zeta-1)(\zeta-2)\, zx^3 + 3\zeta(\zeta-1)\, zx^2 + \zeta zx \end{aligned} \tag{A3}$$

where we have first assumed the probabilities to be independent of the site and then approximated the probability of a cluster by the product of the probabilities of each site.

The second and third terms on the right side of Eq. (A1), proportional to n_i^2 and to n_i respectively, are calculated analogously and the result is

$$\langle \delta(\sigma_i, 0)\, 3n_i^2 \rangle = 3\zeta(\zeta-1)\, zx^2 + 3\zeta zx, \tag{A4}$$

$$\langle \delta(\sigma_i, 0)\, 2n_i \rangle = 2\zeta zx. \tag{A5}$$

When Eqs. (A3)–(A5) are substituted back into Eq. (A1), several terms cancel and we get simply

$$\langle \delta(\sigma_i, 0)\, n_i(n_i-1)(n_i-2) \rangle = \zeta(\zeta-1)(\zeta-2)\, zx^3 \tag{A6}$$

which is exactly the term proportional to $g^3/3!$ in Eq. (27).

APPENDIX B: THE CALCULATION OF χ_1 AND χ_2

In Section 4.3 we noted that Eq. (47) has two possible solutions, one of them used in the text. Here we consider the general solution of (47), show that there are indeed only two possibilities and that only the one considered in Section 4.3 is consistent with the original Eqs. (38) and (39).

Equation (47) has the form $F(x, y) + F(y, x) = 2$. Writing $F(x, y) = 1 + G(x, y)$, then G has to be anti-symmetric, i.e., $G(x, y) = -G(y, x)$.

Making the anti-symmetry explicit we write $F(x, y) = 1 + h(x, y) - h(y, x)$. Therefore, the most general solution of (47) is

$$\begin{aligned} f(\alpha_1, \alpha_2)\, g(\alpha_1)[1-(1-\alpha_1)^\zeta] + (1-\alpha_1)^\zeta &= 1 + h(\alpha_1, \alpha_2) - h(\alpha_2, \alpha_1) \\ f(\alpha_1, \alpha_2)\, g(\alpha_2)[1-(1-\alpha_2)^\zeta] + (1-\alpha_2)^\zeta &= 1 + h(\alpha_2, \alpha_1) - h(\alpha_1, \alpha_2). \end{aligned} \tag{B1}$$

Passing the second term on the left side of each of these equations to the right and dividing one by the other we get

$$\frac{g(\alpha_1)}{g(\alpha_2)}\,\frac{1-(1-\alpha_1)^\zeta}{1-(1-\alpha_2)^\zeta} = \frac{1 + h(\alpha_1, \alpha_2) - h(\alpha_2, \alpha_1) - (1-\alpha_1)^\zeta}{1 + h(\alpha_2, \alpha_1) - h(\alpha_1, \alpha_2) - (1-\alpha_2)^\zeta}. \tag{B2}$$

The left side of (B2) is a quotient of the same function calculated at α_1 and α_2. The right side must, therefore, also be such a quotient. There are three ways in which this may happens: (a) $h(\alpha_1, \alpha_2) = 0$, (b) $h(\alpha_1, \alpha_2) = h(\alpha_2, \alpha_1)$, and (c) $h(\alpha_1, \alpha_2) = \bar{h}(\alpha_1) = (1-\alpha_1)^\zeta$. The first two cases lead to the situation explored in Section 4.3, i.e., $g(\alpha_i) = c$, $f(\alpha_1, \alpha_2) = 1/c$. The third leads to

$$\begin{aligned} f(\alpha_1, \alpha_2)\, g(\alpha_1)[1-(1-\alpha_1)^\zeta] + (1-\alpha_1)^\zeta &= 1 - (1-\alpha_2)^\zeta + (1-\alpha_1)^\zeta \\ f(\alpha_1, \alpha_2)\, g(\alpha_2)[1-(1-\alpha_2)^\zeta] + (1-\alpha_2)^\zeta &= 1 - (1-\alpha_1)^\zeta + (1-\alpha_2)^\zeta. \end{aligned} \tag{B3}$$

Solving for $f(\alpha_1, \alpha_2)\, g(\alpha_1)$ and $f(\alpha_1, \alpha_2)\, g(\alpha_2)$ and dividing one equation by the other we find

$$g(\alpha) = [1-(1-\alpha)^\zeta]^{-2} \tag{B4}$$

and $f(\alpha_1, \alpha_2) = [1-(1-\alpha_1)^\zeta][1-(1-\alpha_2)^\zeta]$. This gives

$$\begin{aligned} \chi_1 &= \left(\frac{1-(1-\alpha_2)^\zeta}{1-(1-\alpha_1)^\zeta}\right)\frac{[1-(1-\alpha_1-\alpha_2)^\zeta]}{2-(1-\alpha_1)^\zeta-(1-\alpha_2)^\zeta} \\ \chi_2 &= \left(\frac{1-(1-\alpha_1)^\zeta}{1-(1-\alpha_2)^\zeta}\right)\frac{[1-(1-\alpha_1-\alpha_2)^\zeta]}{2-(1-\alpha_1)^\zeta-(1-\alpha_2)^\zeta}. \end{aligned} \tag{B5}$$

Now we show that these results are inconsistent: in the limit of small τ_1 and τ_2, χ goes to 1. Therefore, in this limit, both χ_1 and χ_2 should go to 1. However, from the expressions above, $\chi_1 \to \tau_2/\tau_1$ and $\chi_2 \to \tau_1/\tau_2$. This possibility is therefore ruled out and only the one explored in Section 4.3 is valid.

ACKNOWLEDGEMENTS

It is a pleasure to thank Prof. Tania Tomé for a critical reading of this manuscript. This work was supported in part by the National Science Foundation under Grant No. 0083885. M.A.M.A. acknowledges financial support from the Brazilian agencies FAPESP and CNPq.

REFERENCES

1. D. Tilman and P. Kareiva, *Spatial Ecology: The Role of Space in Population Dynamics and Interspecific Interactions* (Princeton University Press, Princeton, NJ, 1997).
2. H. Sayama, L. Kaufman, and Y. Bar-Yam, *Phys. Rev. E* **62**:7065 (2000)
3. H. Sayama, M. A. M. de Aguiar, Y. Bar-Yam, and M. Baranger, *Phys. Rev. E* **65**:051919 (2002)
4. E. M. Rauch, H. Sayama, and Y. Bar-Yam, *Phys. Rev. Lett.* **88**:228101 (2002)
5. E. M. Rauch, H. Sayama, and Y. Bar-Yam, *J. Theor. Biol.* **221**:655 (2003).
6. Y. Bar-Yam, *Dynamics of Complex Systems* (Perseus Books, Cambridge, Massachusetts, 1997).
7. A. Okubo, *Diffusion and Ecological Problems: Mathematical Models* (Springer-Verlag, New York, 1980).
8. M. Gyllenberg, K. Parvinen, and U. Dieckmann, *J. Math. Biol.* **45**:79 (2002)
9. K. Tainaka, *J. Phys. Soc. Japan* **57**:2588 (1988).
10. H. N. Comins, M. P. Hassell, and R. M. May, *J. Anim. Ecol.* **61**:735–748 (1992).
11. M. P. Hassell, H. N. Comins, and R. M. May, *Nature* **370**:290 (1994).
12. K. Sato, H. Matsuda, and A. Sasaki, *J. Math. Biol.* **32**:251–268 (1994).
13. D. A. Rand, M. J. Keeling, and H. B. Wilson, *Proc. R. Soc. London B* **259**:55 (1995).
14. Y. Haraguchi and A. Sasaki, *J. Theor. Biol.* **203**:85 (2000).
15. M. J. Keeling, in *The Geometry of Ecological Interactions*, U. Dieckmann, R. Law, and A. J. Metz, eds. (Cambridge University Press, 2000).
16. Y. Iwasa, in *The Geometry of Ecological Interactions*, U. Dieckmann, R. Law, and A. J. Metz, eds. (Cambridge University Press, 2000).
17. D. A. Rand, in *Advanced Ecological Theory*, J. MacGlade, ed. (Blackwell Science, 1999).
18. J. E. Satulovsky and T. Tome, *Phys. Rev. E* **49**:5073 (1994).
19. M. A. M. de Aguiar, E. M. Rauch, and Y. Bar-Yam, *Phys. Rev. E* **67**:047102 (2003).
20. M. P. Hassell, H. N. Comins, and R. M. May, *Nature (London)* **370**:290 (1994).
21. M. Boots and A. Sasaki, *Ecol. Lett.* **3**:181 (2000).
22. N. J. Savill and P. Hogeweg, *Proc. R. Soc. London B* **265**:25 (1998).
23. M. van Baalen, in *The Geometry of Ecological Interactions*, U. Dieckmann, R. Law, and A. J. Metz, eds. (Cambridge University Press, 2000).
24. H. Mamada and F. Takano, *J. Phys. Soc. Jpn.* **25**:675 (1968).
25. R. Kikuchi, *Phys. Rev.* **81**:988 (1951).
26. R. Dickman, *Phys. Rev. A* **34**:4246 (1986).